JOURNAL OF MATERIALS SCIENCE 18 (1983) 884–893

Computer simulation of polyethylene crystals

Part 3 *The core structure of dislocations*

D. J. BACON, K. THARMALINGAM
Department of Metallurgy and Materials Science, The University of Liverpool, P.O. Box 147, Liverpool, UK

A simulation by computer of dislocations in orthorhombic polyethylene has been undertaken using the DEVILS suite of programs described in Part 1 [2]. The perfect dislocations with the shortest Burgers vector **b** have been considered, namely the screw with **b** = [0 0 1] and the edges with **b** = [0 1 0], [1 0 0] and ⟨1 1 0⟩. The ⟨1 1 0⟩ edge dissociates into Shockley partials with a very wide spacing and could not be modelled successfully with the crystal sizes employed. The other dislocations have narrow cores, and the [0 0 1] screw is symmetrical except for small molecular rotations along the (1 0 0) plane. Under applied shear strain, the screw glides on (1 0 0), (0 1 0) and {1 1 0}, with the [0 0 1] (1 0 0) system having the lowest Peierls stress. The [1 0 0] and [0 1 0] edge dislocations are not glissile on their slip planes, however. Instead of gliding on (0 1 0), the [1 0 0] edge dissociates under stress in a non-planar way on the {1 1 0} planes. It is predicted that transverse slip in polyethylene occurs by combinations of partial dislocation glide on the two {1 1 0} planes.

1. Introduction

The variety of slip, twinning and martensitic-transformation modes by which polymer crystals can deform by shear was discussed in Part 2 [1]. As explained there, a full understanding of the mechanical properties of crystalline polymers requires detailed knowledge of the molecular distortions and displacements around the dislocations and interfaces associated with these modes. This information demands a theoretical approach, the most straight-forward at the moment being crystal simulation by computer. The DEVILS suite of programs described in Part 1 [2], was used in Part 2 to simulate stacking-fault and twin-boundary interfaces in model polyethylene crystals, and it has been applied for the present work to the simulation of dislocation-core structures.

DEVILS employs the crucial assumption that the individual molecular chains are infinitely-long and rigid, so that intramolecular distortions and surface effects, such as molecular folds, are neglected. With this assumption, the computation of the required lattice sums becomes tractable, and for dislocations it means that only those which are infinite in length and lie along the [0 0 1] chain-axis direction can be modelled. This is not as restrictive and it might at first appear, for dislocations which result in broken covalent bonds are unlikely to occur, and those which leave bonds intact but distorted appear from indirect evidence to play an insignificant role in deformation [1]. The dislocations considered here, therefore, lie along [0 0 1] and are responsible for slip on planes of the [0 0 1] zone. Their Burgers vectors are the four shortest, distinct lattice vectors of the orthorhombic form of polyethylene, namely [0 0 1], [0 1 0], [1 0 0] and ⟨1 1 0⟩; the first of these defines the screw dislocation believed to be responsible for "chain-axis slip", whereas the other three belong to the edge dislocations that are anticipated to be dominant in "transverse slip". (The monoclinic phase was not considered in this part of the study.)

The molecular configuration within the core region of these dislocations has been simulated using the methods outlined in Part 1. Dislocations

0022–2461/83/030884–10$03.70/0

have been modelled in crystals either free of external stress or strained homogeneously as if under an externally applied shear stress. The stress in the latter state was chosen to act on the slip plane in the direction of the Burgers vector, and therefore induces the dislocation to move by glide.

2. Methods

Crystallites of orthorhombic polyethylene were set up in the form of rectangular parallelepipeds using the lattice-handling routines of DEVILS [2]. The block edges were chosen to be parallel to [1 0 0], [0 1 0] and [0 0 1], referred to here x, y, z, respectively. The molecular chains were infinitely long in the z direction, and blocks containing up to 160 chains in the inner, relaxable region were generated. The outer mantle of fixed molecules surrounding the x and y faces was of sufficient thickness to ensure that all molecules of the inner region had a full set of neighbours consistent with the range of the interatomic potentials used. The main dislocations investigated are shown schematically in Fig. 1. A dislocation was introduced into a perfect crystallite by imposing the displacements of linear elasticity theory on the molecules of the inner and outer regions. The dislocation displacements given by anisotropic elasticity [3] with the elastic constants appropriate to the interatomic potential [2] were used for the screw (Fig. 1a), whereas the approximation of isotropic elasticity with an effective Poisson's ratio calculated from the anisotropic energy factors was adopted for the edges (Fig. 1b and c). The effects of imposed anisotropy within the outer region on the relaxed displacements in the core were found to be insignificant for the block sizes used.

The molecules were allowed to interact via the Williams set I potentials with ranges extended as discussed in Part 1. Most relaxation runs employed fewer than 160 inner-region chains in order to reduce computer time, but in all cases the final runs used crystallites of this size in order to ensure that the rigid boundaries did not influence the relaxed core structure. In particular, small variations in the dislocation origin selected for the initial elastic displacements had an insignificant influence on the relaxed displacements for the block sizes chosen.

To induce the model dislocations to move by slip, a simple, homogeneous, shear strain was applied to the molecules of the inner and outer regions of the fully-relaxed crystallite, which was then relaxed again. The [0 0 1] screw (Fig. 1a) can, in principle, slip on any plane of the [0 0 1] zone, but only the low-index, most widely-spaced planes were considered, i.e. (1 0 0), (0 1 0) and (1 1 0). The simple shears applied were therefore e_{31}, e_{32} and $e_{32'}$, respectively, where subscript 2′ refers to the (1 1 0) plane. (In the notation adopted here, e_{31}, for example, is a shear in the z direction on a plane normal to the x-axis.) The shears applied for [0 1 0](1 0 0) and [1 0 0](0 1 0) slip of the two edge dislocations of Fig. 1b and c were e_{21} and e_{12}, respectively. If linear elasticity is assumed to describe the response of a crystallite to stress, the shear stress resulting in the shear strain e is μe, where μ is the appropriate shear modulus as computed in Part 1, i.e. C_{55}, C_{44}, C_{66} and C_{66} for the slip systems [0 0 1](1 0 0), [0 0 1](0 1 0), [0 1 0](1 0 0) and [1 0 0](0 1 0), respectively, and a combination of C_{44} and C_{55} for [0 0 1](1 1 0) slip. However, it will be seen later that the strains required for slip are large, so that μe is only a poor approximation to the stress. In the following, therefore, strain rather than stress values are quoted.

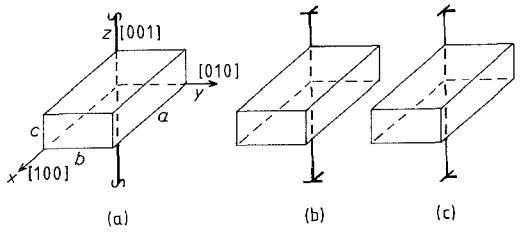

Figure 1 Geometric representation of the dislocations studied showing their relationship to the lattice unit cell, which has parameters a, b, c. The Burgers vectors are (a) [0 0 1], (b) [0 1 0] and (c) [1 0 0].

3. Results for unstressed crystals

3.1. Edge dislocations

The relaxed molecular configuration in crystals containing the edge dislocations with Burgers vector **b** (not to be confused with lattice parameter b) equal to [0 1 0] and [1 0 0] is shown by the computer-generated symbols in Fig. 2a and b. The positions of the molecules and their setting angles are denoted by the vector arrows, as defined in Part 1. No displacements have occurred in the [0 0 1] z-axis direction normal to the plane of the figures. It can be seen that the two extra half-planes of the [0 1 0] edge are mainly accommodated

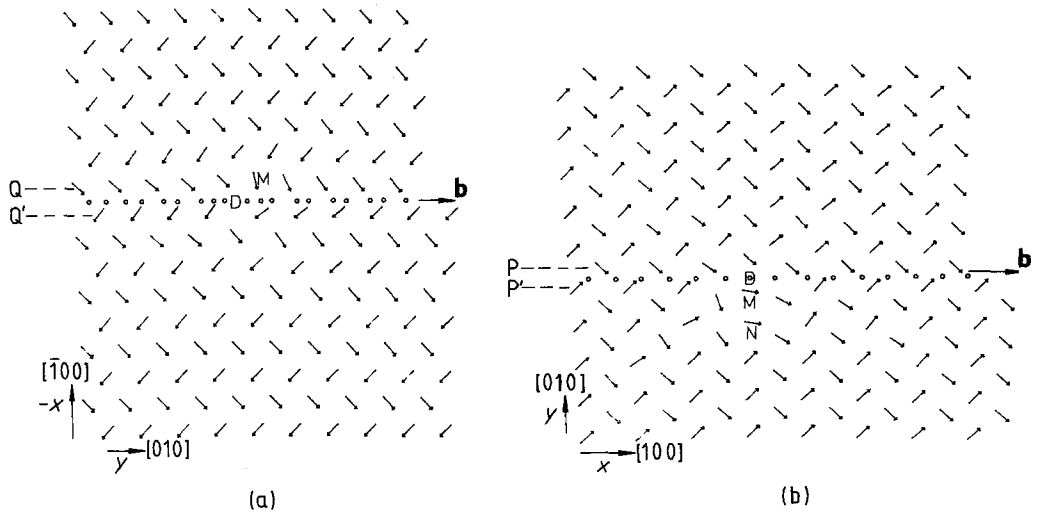

Figure 2 Relaxed molecular positions and orientations for the edge dislocations with Burgers vector **b** equal to (a) [0 1 0] and (b) [1 0 0].

in a narrow region of the (1 0 0) slip plane. Only a few molecules undergo significant rotations, the largest being 29° and taking place at the bottom of one of the half-planes labelled M in Fig. 2a. The two half-planes of the [1 0 0] edge in Fig. 2b are likewise accommodated without widespread disruption of coordination across most of the slip plane. This is only achieved, however, by both half-planes consisting effectively of molecules of setting angle + 43°, the half-plane between them with chains of setting angle − 43° forming a continuous plane with chains of angle + 43° below the slip plane. In the transition region on this plane, i.e. within the dislocation core, considerable chain rotations occur, the largest being 53° for the molecules labelled M and N in Fig. 2b.

A useful way of representing the molecular displacements in cores of this type is to plot the relative displacements in the direction of **b** between molecules on opposite sides of the slip plane as a function of position along the slip plane: i.e. to plot Δu_y against y for the [0 1 0] edge of Fig. 2a and Δu_x against x for the [1 0 0] edge of Fig. 2b. These functions are shown by the Δu (relaxed) curves in Fig. 3a and b, respectively: each data point was obtained from the pairs of molecules in the planes labelled PP′ and QQ′ in Fig. 2 and whose mean positions are marked by small circles along the slip plane. (The displacements used to calculate these plots were those of the chain-centre axes, and chain rotation effects are, therefore, neglected.) The curves rise from approximately zero to a value close to $|\mathbf{b}|$ − equal to the lattice parameters b and a for the two dislocations, respectively − as the core is traversed along the slip plane: the faster the rise the narrower the core. An even more effective way of indicating graphically the structure of the core is to plot the derivatives of the displacement differences [4], i.e.

$$\rho_x(x) = \frac{\partial}{\partial x}(\Delta u_x), \quad \rho_z(x) = \frac{\partial}{\partial x}(\Delta u_z),$$

$$\rho_y(y) = \frac{\partial}{\partial y}(\Delta u_y), \quad \text{etc.}$$

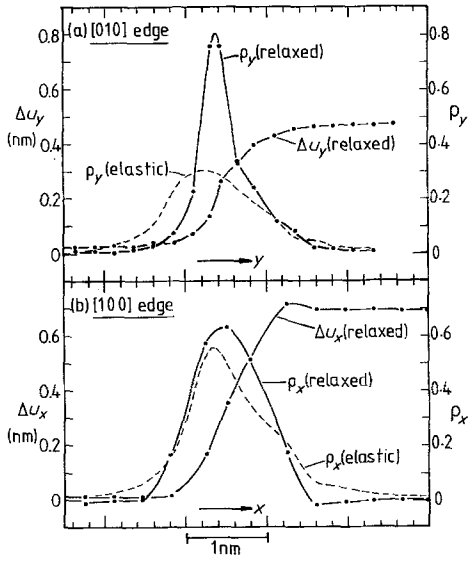

Figure 3 The displacement differences Δu and Burgers vector distribution function ρ along the slip plane of the edge dislocations with **b** equal to (a) [0 1 0] and (b) [1 0 0].

These functions give a continuous representation of the distribution of Burgers vector along the slip plane, for, taking the [1 0 0] edge as an example,

$$\int_{-\infty}^{\infty} \rho_x(x)\,dx = |\mathbf{b}|, \quad \int_{-\infty}^{\infty} \rho_z(x)\,dx = 0.$$

Only in the case of dissociation within the core into partial dislocations with screw component will the density functions $\rho_z(x)$ and $\rho_z(y)$ be non-zero; that did not occur in the present study as the displacements u_z were zero.

The derivative at any one datum point on the Δu plots of Fig. 3 was computed from the gradient there of the quadratic fitted through the point and the adjacent point on each side. The resulting Burgers vector distributions are shown by the curves labelled ρ_y (relaxed) and ρ_x (relaxed) in Fig. 3a and b, respectively. The y and x positions of the peaks on these two curves are denoted by the D symbols on the molecule plots of Fig. 2.

For purposes of comparison, the initial, unrelaxed distribution of Burgers vector, ρ (elastic), is also shown in the two figures. It can be seen that both ρ (relaxed) curves exhibit a single, well-defined peak; this is to be expected in the absence of stable stacking faults [1] (and therefore dislocation dissociation) on the (1 0 0) and (0 1 0) planes of orthorhombic polyethylene. A striking feature of the [0 1 0] edge, however, is that molecular relaxation actually reduces the width of the core, thereby restricting the zone of disregistry over which Δu changes from zero to $|\mathbf{b}|$ to a narrow region of slip plane. There is a similar, but less marked, effect for the [1 0 0] edge.

The third edge dislocation referred to in Section 1 has a Burgers vector $\mathbf{b} = \langle 1\,1\,0 \rangle$. Despite the fact that this vector is much longer than the others, thereby implying a large lattice energy associated with the dislocation, the structure of the $\{1\,1\,0\}$ planes is such that the dislocation can dissociate into two Shockley partials bounding a ribbon of stacking fault. Several stable, translational faults exist on the $\{1\,1\,0\}$ planes [1], and the dissociation most favoured by Frank's rule is

$$\langle 1\,1\,0 \rangle \rightarrow \langle 0.47\ 0.47\ 0 \rangle + \langle 0.53\ 0.53\ 0 \rangle, \quad (1)$$

resulting in a reduction in $|\mathbf{b}|^2$ of 50%. The stacking-fault energy of the enclosed fault is 12.5 mJ m^{-2} according to the simulations reported in [1], and the corresponding partial spacing calculated from elasticity theory using the model elastic constants given in [2] is 33 nm. This width is much too large to permit the dissociated dislocation to be simulated in a computer model, although a perfect $\langle 1\,1\,0 \rangle$ dislocation was introduced in one experiment to ensure that dissociation would actually occur. It did, the partials which formed during relaxation moving apart until constrained by the boundary between the inner and outer (rigid) regions and bounding a stacking fault as defined in Reaction 1.

3.2. Screw dislocation

The positions and setting-angle vectors for the molecules of the inner region used for the c-axis screw dislocation are shown in Fig. 4. (This, of course, is also the perfect crystallite used for the edge simulations.) During relaxation to minimize the energy, the molecular movements in the x and y directions were small, being less than 0.1 Å in all cases. The rotations were also small, the largest being those of chains labelled A, B, C, D, which rotated anti-clockwise by 1°, 4°, 2.5° and 0.5°, respectively, and E, F. G, which rotated clockwise by 2°, 4.5° and 2°, respectively; all other rotations were less than 0.3°. The molecular rotations associated with the screw are therefore largely accommodated on the (1 0 0) plane. The distribution of the z-axis displacements u_z in the core have been monitored for the low-index planes through the core centre, i.e. (0 1 0), (0 0 1) and (1 1 0). The displacement differences Δu_z between pairs of molecules in these planes (labelled PP′, QQ′ and RR′ in Fig. 4) have therefore been determined, the mean position of each pair considered

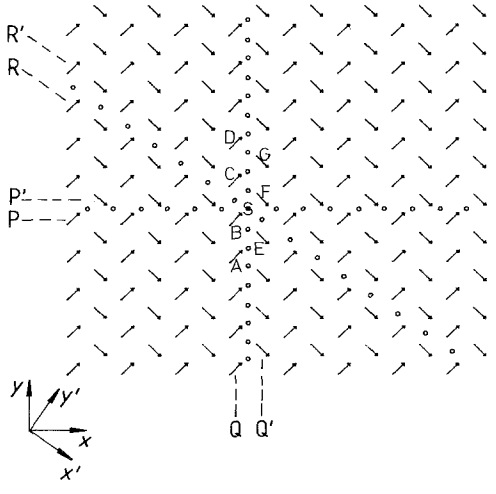

Figure 4 The inner, relaxable region of the crystallite employed for the simulation of the [0 0 1] screw dislocation.

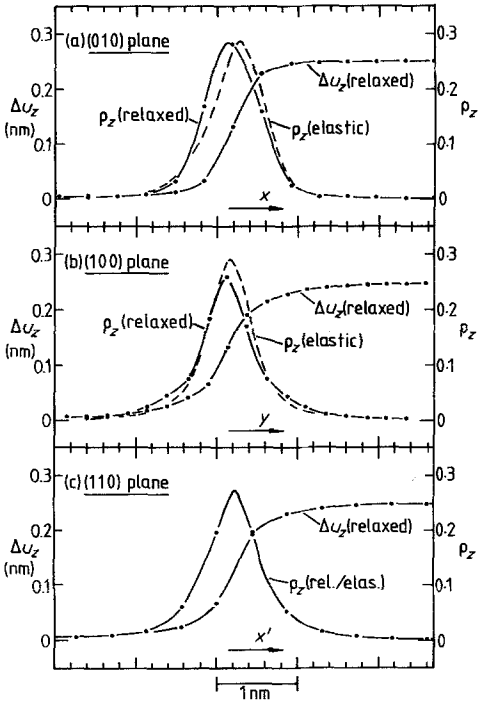

Figure 5 The displacement differences Δu and Burgers vector distribution function ρ along (a) the (0 1 0) planes PP', (b) the (1 0 0) planes QQ' and (c) the (1 1 0) planes RR' through the core of the [0 0 1] screw dislocation.

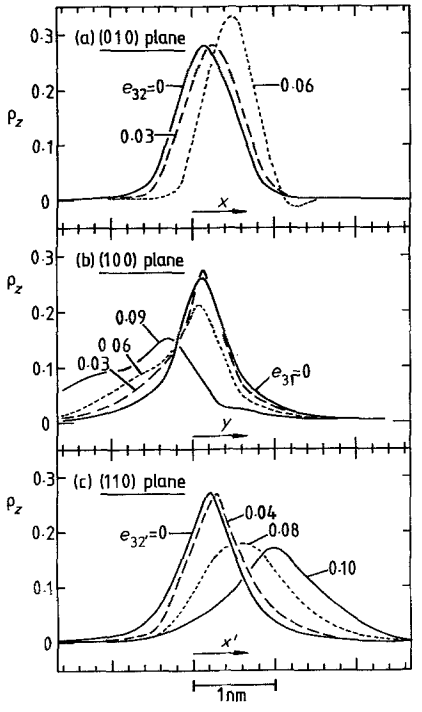

Figure 6 The Burgers vector distribution function along the low-index slip planes of the [0 0 1] screw dislocation for applied shear strains e less than the critical value.

being shown as a small circle in the figure. The distribution of Burgers vector on each plane was then calculated from the relations

$$\rho_z(x) = \frac{\partial}{\partial x}(\Delta u_z), \quad \rho_z(y) = \frac{\partial}{\partial y}(\Delta u_y),$$

$$\rho_z(x') = \frac{\partial}{\partial x'}(\Delta u_z),$$

where x' is the direction lying along RR', as indicated in Fig. 4. The resulting Δu and ρ plots for the relaxed and unrelaxed, i.e. elastic, configurations are given in Fig. 5a to c.

The ρ plots show a single peak located at the point marked S in Fig. 4, indicating that the screw dislocation does not dissociate in any of the three planes. In fact, the change in core width, as measured, say, by the "width at half-peak height" of the ρ curves, is almost unchanged by relaxation in each case. The widest core occurs on the (0 1 0) plane, but this is mainly a manifestation of the interplanar spacing, as seen by the elastic solution, and is not significant.

4. Results for stressed crystals

4.1. Screw dislocation

The state of the dislocation core was monitored after each increment of applied strain both by direct inspection of plots of the molecular configuration and by computation of the Δu and ρ values along the slip plane. The critical strain for slip, which is the Peierls stress divided by μ, is taken here to be the value of applied strain for which the peak of the Burgers vector distribution is displaced by one lattice repeat distance along the slip plane. For larger strains than this, the dislocation moves by several repeat distances until the restraining influence of the (unrelaxed) molecules in the outer region is encountered. The results for the [0 0 1] screw dislocation are easiest to describe and are considered first.

Plots of the Burgers vector distribution ρ_z along the slip plane for various values of applied shear strain e less than the critical value are shown in Fig. 6. The strains applied were e_{32}, e_{31} and $e_{32'}$ for the (0 1 0), (1 0 0) and (1 1 0) slip planes, respectively, where the axes are defined in Figs. 1a and 4. The dislocation simulated is a right-handed screw, and it therefore moves in the $+x$ direction under positive e_{32}, the $-y$ direction under positive e_{31}, and the $+x'$ direction under positive $e_{32'}$. The critical strains for movement were found to be 0.073, 0.092 and 0.105 for the (0 1 0), (1 0 0) and (1 1 0) slip planes, respectively. The molecular

chain rotations at all strains up to and including those for which the dislocation moved were small, never exceeding 5°. It can be seen from the ρ curves that the shift and shape changes in the core distribution are small until the strain is at least half the critical value. It is at first surprising that the critical strain for [0 0 1](1 0 0) slip is not the lowest, for in the unstressed crystal the core of the screw dislocation seems to be accommodated by small chain rotations on either side of this plane (Section 3.2) and the (1 0 0) planes have the widest interplanar spacing in the structure. It is apparent from Fig. 6, however, that whereas the ρ curves for the (0 1 0) and (1 1 0) planes retain a fairly symmetrical shape until slip occurs, the profile on (1 0 0) becomes very broad in nature. For this reason, the precise value of the critical strain for the latter case is less certain than for the other systems. If the critical strain is defined not as above, but from the displacements of either the point $\Delta u_z = |\mathbf{b}|/2$ on the Δu_z plot or the centre of gravity of the ρ_z plot, its value is reduced to less than 0.08. Bearing in mind the smaller value of the transverse shear modulus for the (1 0 0) plane, i.e. $C_{55} < C_{44}$ [2], it is probably safe to conclude that the [0 0 1](1 0 0) system has the smallest Peierls stress for chain-axis slip.

4.2. Edge dislocations

Under a positive applied strain e_{21}, the [0 1 0] edge dislocation of Fig. 2a experiences a force to the left, and under positive strain e_{12}, the [1 0 0] edge of Fig. 2b tends to move to the right. The distribution of Burgers vector in the (1 0 0) and (0 1 0) slip planes for increasing values of these strains is given in Fig. 7a and b, respectively. It can be seen that rather than widen and shift as expected, the cores actually become narrower with no tendency for slip to occur. Even by applying strains as large as 0.16, the dislocated crystals could not be induced to slip on the [0 1 0](1 0 0) and [1 0 0](0 1 0) systems.

The explanation for this behaviour is best sought in the computer-generated plots of the molecular positions. Fig. 8a shows the (0 0 1) projection of the molecules for the edge dislocation with $\mathbf{b} = [1\,0\,0]$, as first given in Fig. 2b. In this case, however, the molecules are depicted not only by vector arrows denoting the plane of the carbon–carbon zig-zag, but also by crosses and asterisks: this has been done to distinguish between chains originally at the orthorhombic unit cell

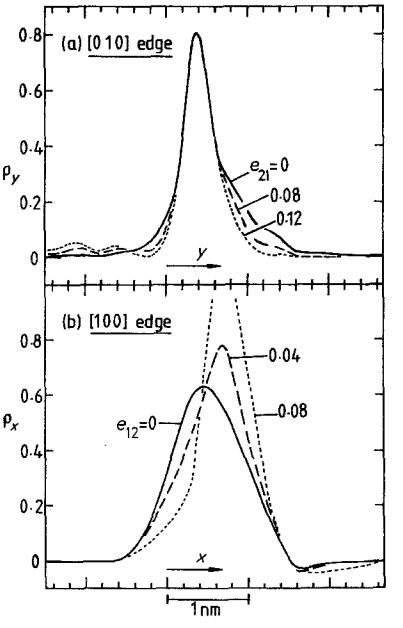

Figure 7 The Burgers vector distribution function along (a) the (1 0 0) slip plane for the [0 1 0] edge, and (b) the (0 1 0) slip plane for the [1 0 0] edge. The values of e of the applied strains e_{21} in (a) and e_{12} in (b) are indicated.

corners (crosses) and those at the unit cell centres (asterisks). It is now easier to visualize the [1 0 0] edge dislocation, not only as two extra (1 0 0) half-planes, but also as two extra {1 1 0} half-planes. The latter planes have indices (1 1 0) and (1 $\bar{1}$ 0), and are labelled A and B in Fig. 8a; the centre of the dislocation core is defined by the letter D. Fig. 8b shows the same crystallite under an applied strain e_{12} of 0.12. By viewing the figure along the [0 1 0], [1 1 0] and [1 $\bar{1}$ 0] directions, it may be seen that slip has occurred, but not on the (0 1 0) plane. The effective extra {1 1 0} half-planes have moved under the strain to the new positions labelled A and B, and the perfect dislocation with slip plane (0 1 0) has dissociated into two partial dislocations labelled D_1 and D_2. The slip planes of the partials are (1 $\bar{1}$ 0) and (1 1 0), respectively. The partial D_1 is quite distinct, and by its glissile motion along (1 $\bar{1}$ 0) a stacking fault (denoted by a dashed line) has been produced, as clearly seen by the relative positions of the crosses and asterisks.

It was reported in Part 2 [1] that for the model crystallite used in this work, several stable stacking faults can exist on the {1 1 0} planes. One has an energy of 12.5 mJ m^{-2} and translation vectors of 0.47 [1 $\bar{1}$ 0] on (1 1 0) and 0.53 [1 1 0] on (1 $\bar{1}$ 0); the others include an additional translation

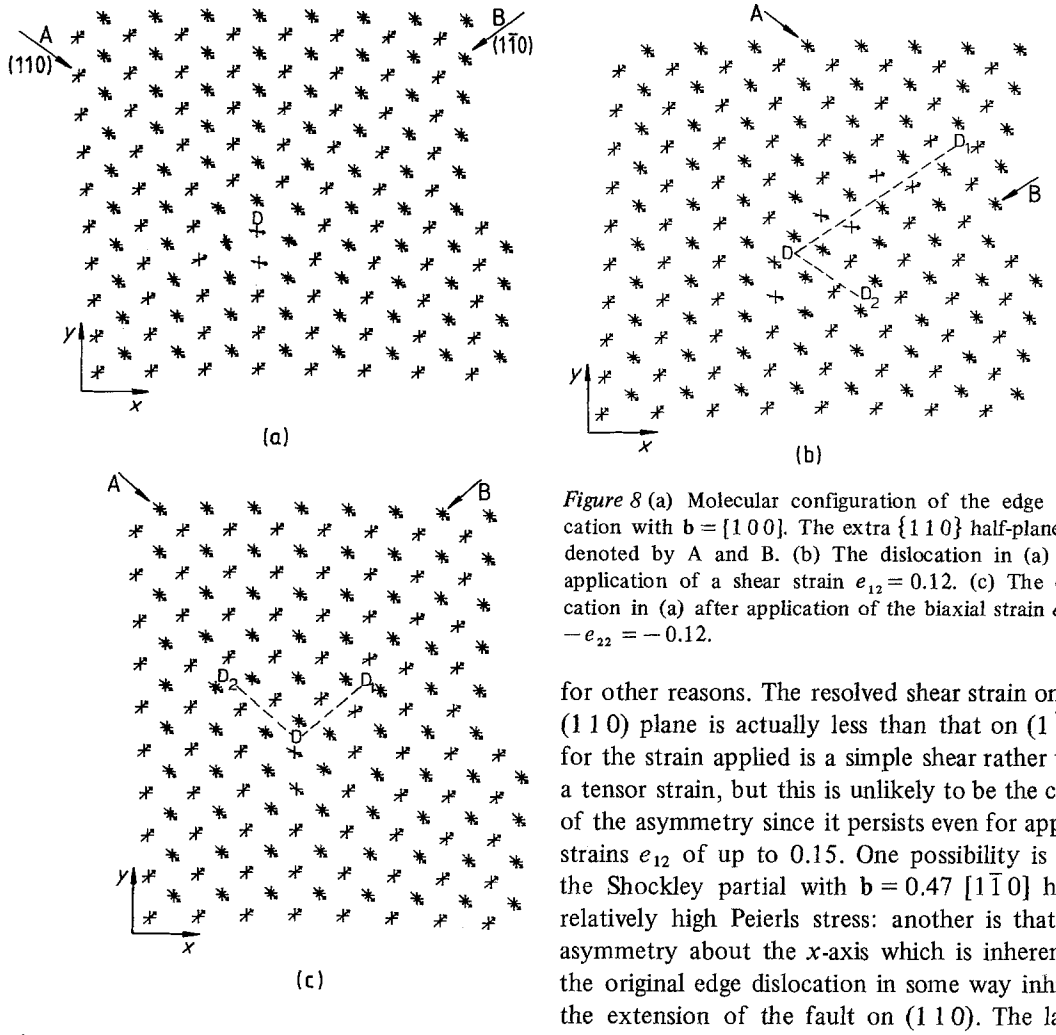

Figure 8 (a) Molecular configuration of the edge dislocation with $\mathbf{b} = [1\,0\,0]$. The extra $\{1\,1\,0\}$ half-planes are denoted by A and B. (b) The dislocation in (a) after application of a shear strain $e_{12} = 0.12$. (c) The dislocation in (a) after application of the biaxial strain $e_{11} = -e_{22} = -0.12$.

of $\frac{1}{2}$ [0 0 1], and are not involved here. (The translations given refer to shifts of the material above the fault plane relative to the material below.) From its appearance in Fig. 8b, the fault between D and D_1, has a translation vector close to $\frac{1}{2}$ [1 1 0], although it is not sufficiently extended to be undistorted by the dislocation core.* However, if it is taken to be 0.53 [1 1 0], i.e. D_1 has a Burgers vector of 0.53 [1 1 0], the reaction involved in the dissociation has the form

$$[1\,0\,0] \rightarrow 0.53\,[1\,1\,0] + 0.47\,[1\,\bar{1}\,0] + 0.06\,[0\,\bar{1}\,0]. \quad (2)$$

Glide of D_1 appears from Fig. 8b to be restrained by the fixed molecules in the outer region surrounding the crystallite, whereas D_2 must have stopped for other reasons. The resolved shear strain on the (1 1 0) plane is actually less than that on (1 $\bar{1}$ 0), for the strain applied is a simple shear rather than a tensor strain, but this is unlikely to be the cause of the asymmetry since it persists even for applied strains e_{12} of up to 0.15. One possibility is that the Shockley partial with $\mathbf{b} = 0.47\,[1\,\bar{1}\,0]$ has a relatively high Peierls stress: another is that the asymmetry about the x-axis which is inherent in the original edge dislocation in some way inhibits the extension of the fault on (1 1 0). The latter interpretation is supported by the values of the displacement differences between the molecules on the neighbouring $\{1\,1\,0\}$ planes which pass through the core centre D: even in the unstressed crystal, the core displacements are more widely spread in the upward-pointing [1 1 0] and [$\bar{1}$ 1 0] directions than the downward-pointing [1 $\bar{1}$ 0] and [$\bar{1}$ $\bar{1}$ 0] directions. Furthermore, when a negative strain e_{12} is applied, the dissociation again becomes asymmetrical, one Shockley partial gliding upwards on (1 1 0) creating a stacking fault, the other on (1 $\bar{1}$ 0) remaining close to the stair-rod at D. The Burgers vector reaction in this second case is

$$[1\,0\,0] \rightarrow 0.53\,[1\,\bar{1}\,0] + 0.47\,[1\,1\,0] + 0.06\,[0\,1\,0]. \quad (3)$$

*It is of interest to note that the fault produced by D_1 is not a pure translation fault, for some of the molecules adjacent to the fault (denoted by crosses) have been rotated. A number of metastable faults of this type probably exist with similar energies, and the one in Fig. 8b may revert to the pure translation form if D_1 were allowed to move away.

The core structure of the [1 0 0] edge dislocation can therefore be imagined as having a "vee" form, the principal displacement differences being accommodated on the two arms of the vee which point upwards (for a positive edge) along the (1 1 0) and (1 $\bar{1}$ 0) planes. These displacements form the embryos of two Shockley partials having Burgers vectors 0.53 [1 $\bar{1}$ 0] on (1 1 0) and 0.53 [1 1 0] on (1 $\bar{1}$ 0). The dislocation can be induced to dissociate in a symmetrical manner by applying equal shears symmetrically on the two {1 1 0} planes of the vee. This is demonstrated in Fig. 8c, which is the molecular configuration resulting from the application of a biaxial strain $e_{11} = -e_{22} = -0.12$ to the crystallite of Fig. 8a. In this situation, the two Shockley partials have moved approximately equal distances from D along the (1 1 0) and (1 $\bar{1}$ 0) planes, and the Burgers vectors involved in the dissociation are

$$[1\,0\,0] \rightarrow 0.53\,[1\,\bar{1}\,0] + 0.53\,[1\,1\,0] + 0.06\,[\bar{1}\,0\,0]. \quad (4)$$

From this result, it would appear that under the application of a simple shear e_{12} (positive or negative), one Shockley partial moves away from D and extends the fault, and the other glides back into D to combine with the 0.06 [$\bar{1}$ 0 0] stair-rod partial and then react as described in either Reaction 2 or 3: the second Shockley thus formed is unable for some reason to move freely away from the vicinity of D. All the reactions described in Reactions 2, 3 and 4 are energetically favourable according to Frank's rule.

Finally, the molecular structure of the edge dislocation with $\mathbf{b} = [0\,1\,0]$, as shown in Fig. 2a, has been examined to see if there is any tendency for this core also to adopt a non-planar form. None was found. Even under large shear strains e_{21}, the core retains an almost unaltered form, as is clear from the curves of Fig. 7a. The effective extra {1 1 0} half-planes remain those which can be discerned in Fig. 2a, and no partials with ⟨1 1 0⟩ components are formed. The same lack of dissociation was found when strains e_{12} were applied. It is not surprising that this dislocation does not dissociate, for the decomposition of the vector [0 1 0] into components of approximately $\frac{1}{2}$⟨1 1 0⟩ would be energetically unfavourable according to Frank's rule for dislocation reactions. On the other hand, it was anticipated that the [0 1 0] edge would slip on the (1 0 0) plane since the interplanar spacing for this system is the widest in the structure. However, inspection of the stacking-fault-energy surfaces presented in Part 2 [1] shows that there exists on the (1 0 0) plane a very large barrier to the relative displacement of molecules in the [0 1 0] direction. This is believed to be the reason for the narrowness of the dislocation core and the strong resistance to slip, which would require molecules to move past each other in the [0 1 0] direction.

5. Discussion

To test for any marked dependency of the dislocation cores on the precise details of the interatomic potentials employed, unstressed crystals containing the three dislocations of Fig. 1 were relaxed using the set VII potentials defined in Part 1. The resulting forms were not significantly different from those reported in Section 3 on the basis of the set I potentials. A similar result was observed in Part 2 for stacking faults, and it is concluded, therefore, that the molecular configurations obtained here are meaningful and representative of the polyethylene structure.

The strains required to make the dislocations move are large in comparison with values experienced in practice. This is not a block-size effect, for tests were made using different crystallite sizes to ensure that the presence of the rigid boundary regions did not unduly influence the results obtained. Nor is this observation peculiar to polymers, for in a number of simulations of dislocation glide in model metal crystals, critical strains of up to several per cent have been encountered [5]. The answer probably lies in the fact that the computer programs simulate crystals at 0 K, and thermal activation through lattice vibrations would almost certainly reduce the Peierls stress values by orders of magnitude. It is considered that computer modelling gives values which are probably reasonable estimates relative to each other, and, more importantly, shows molecular effects such as dislocation core structure and dissociation that reliably reflect the behaviour of real systems.

The results of Section 3.2 show that the [0 0 1] screw dislocation has a narrow core without any tendency to spread on the planes of the [0 0 1] zone. This confirms the predictions of the study of the stacking-fault-energy surfaces in Part 2. Under the application of shear strains, the dislocation was induced to glide on all the low-index

planes of the zone, the slip systems [0 0 1](1 0 0) and [0 0 1](0 1 0) apparently being most favoured in that order. Experimental evidence with which to compare this result is sparse, although chain-axis slip is known to be an important process in the deformation and drawing of polyethylene [6, 7]. Some experiments have indicated that the critical resolved shear stress (CRSS) is less on (1 0 0) than (0 1 0) and vice versa [6, 7], but, as discussed by Young [8], yield may be controlled by dislocation generation rather than the Peierls stress. The CRSS for (0 1 0) slip measured by Young at 300 K corresponds to a critical shear strain of about 0.01, and from its strong temperature dependence could well rise at low temperatures to the value found here. The present study is, therefore, consistent with the experimental evidence at hand, but is unable to confirm the detail of Young's analysis.

The only other theoretical investigation with which to compare the critical strains reported in Section 4.1 is that of Peterson [9], who also considered a lattice of rigid, infinite chains, but with different, shorter-range potentials from those adopted here. He estimated the Peierls stress by imposing the dislocation displacements of linear elasticity on the lattice, and then calculated the change in lattice energy as the dislocation origin was moved along the slip plane. The stress for (1 0 0) and (0 1 0) slip was found for different values of the ratio C_{44}/C_{55}, for which the model used actually gave the high value of 8.4. Peterson's published curves do not extend to values in the more-reasonable range of 1 to 2, but if extrapolation is permitted, they give critical strains between 0.001 and 0.01 for (1 0 0) slip and 0.01 and 0.04 for (0 1 0) slip. These results again predict that (1 0 0) slip is favoured, and, bearing in mind the limitations of the model, are in reasonable agreement with the more realistic simulations of the present work.

The computer simulations are unambiguous in predicting that if c-axis edge dislocations with **b** equal to [1 0 0] or [0 1 0] exist in polyethylene, they are not glissile and cannot contribute directly to transverse slip: slip on the (0 1 0) and (1 0 0) planes should only occur in the [0 0 1] direction. This was partly anticipated in Part 2 from the shape of the γ-surface for these two planes, for the maximum value of $|\text{grad}\,\gamma|$ is orders of magnitude higher in the transverse directions than in [0 0 1]. It was not anticipated, however, that the **b** = [1 0 0] edge would actually adopt a non-planar form and dissociate on the inclined {1 1 0} planes. The results firmly indicate that transverse slip occurs only on the two ⟨1 1 0⟩{1 1 0} systems, and it would be interesting to know whether the reports of (1 0 0) and (0 1 0) slip inferred from experiments [6, 7] actually arise from combinations of {1 1 0} slip. Transverse slip resulting from dissociated **b** = ⟨1 1 0⟩ dislocations should be very easy, for the maximum gradients on the γ-surface are small [1] and the partial spacing is wide (Section 3.1). Even if it results from the dissociation of the [1 0 0] dislocation as in Section 4.2, the shear stress required to simply extend the stacking fault by the glide of the single Shockley partial should be small: i.e. taking $\gamma = 12.5\,\text{mJ m}^{-2}$ [1], the shear stress $(= 2\gamma/(a^2 + b^2)^{1/2})$ is only approximately 0.01 of the transverse shear modulus on {1 1 0}. (The critical shear strain on the $(1\,\bar{1}\,0)$ plane for glide of the partial D_1 in Fig. 8b was actually 0.03, which reflects the relatively high value of the Peierls resistance at 0 K in the computer simulations.) It may be expected that Shockley partials on the {1 1 0} planes – either singly or in pairs – will be responsible for transverse slip whatever the plane of maximum resolved shear stress. It is interesting to note in support of this that Holland [10] observed a large number of isolated, single, partial dislocations of this form in polyethylene crystals using Moiré-fringe contrast in the transmission-electron microscope.

Finally, the point made in Parts 1 and 2 that crystallite surfaces consisting of chain folds may play a significant part in affecting deformation mechanisms should be re-emphasized. The simulations reported here have deliberately concentrated on the way structural effects within crystals affect dislocation properties. When more detailed information on surface folds is available, it might also be possible to incorporate them into computer models.

Acknowledgements

The authors gratefully acknowledge assistance and discussions from Drs N. A. Geary and A. P. P. Nicholson. The research was supported by a grant from the Science Research Council.

References

1. N. A. GEARY and D. J. BACON, *J. Mater. Sci.* 18 (1983) 853.
2. D. J. BACON and N. A. GEARY, *ibid.* 18 (1983) 864.

3. L. G. SHADRAKE and F. GUIU, *Phil. Mag.* **34** (1976) 565.
4. V. VITEK, L. LEJCEK and D. K. BOWEN, in "Interatomic Potentials and Simulation of Lattice Defects", edited by P. Gehlen, J. R. Beeler, Jr and R. I. Jaffee (Plenum Press, New York, 1971) p. 493.
5. D. J. BACON and J. W. MARTIN, *Phil. Mag.* **A43** (1981) 901.
6. P. B. BOWDEN and R. J. YOUNG, *J. Mater. Sci.* **9** (1974) 2034.
7. R. J. YOUNG, in "Developments in Polymer Fracture – I", edited by E. H. Andrews (Applied Science, London, 1979) Ch. 7.
8. *Idem, Phil. Mag.* **30** (1974) 85.
9. J. M. PETERSON, *J. Appl. Phys.* **39** (1968) 11.
10. V. F. HOLLAND, *ibid.* **35** (1964) 3235.

Received 18 May
and accepted 29 July 1982